

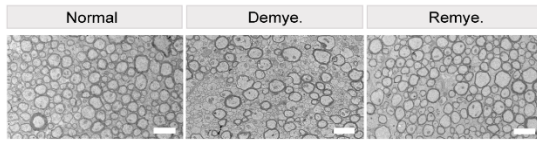
Cell Reports, Volume 42

Supplemental information

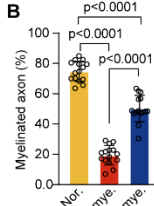
**Transcriptomic atlas and interaction
networks of brain cells in mouse CNS
demyelination and remyelination**

Jinchao Hou, Yingyue Zhou, Zhangying Cai, Marina Terekhova, Amanda Swain, Prabhakar S. Andhey, Rafaela M. Guimaraes, Alina Ulezko Antonova, Tian Qiu, Sanja Sviben, Gregory Strout, James A.J. Fitzpatrick, Yun Chen, Susan Gilfillan, Do-Hyun Kim, Steven J. Van Dyken, Maxim N. Artyomov, and Marco Colonna

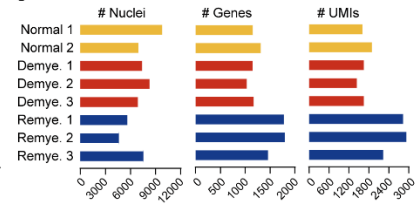
A



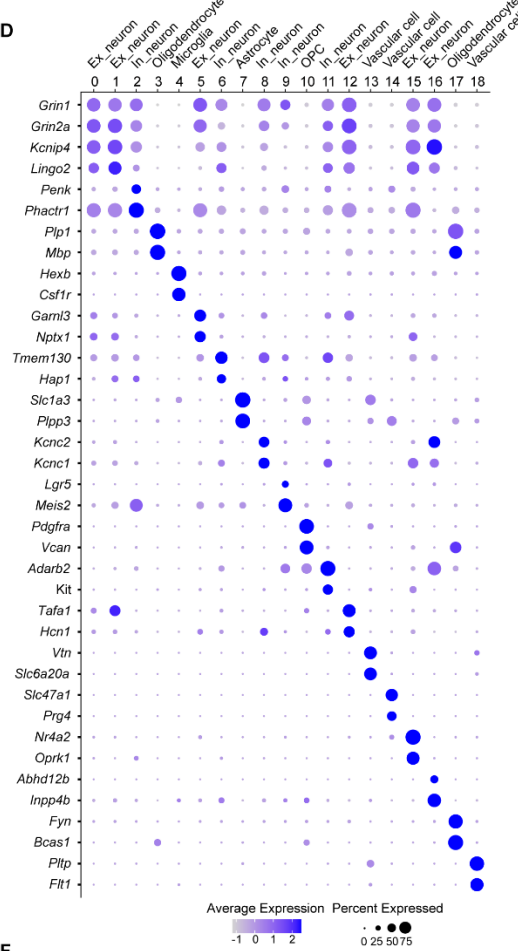
B



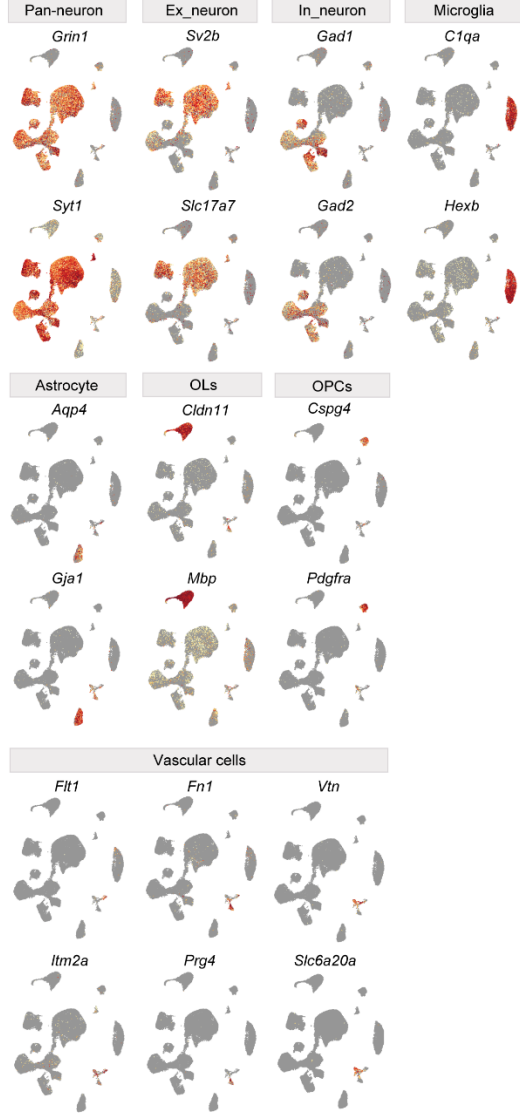
C



D



E



F

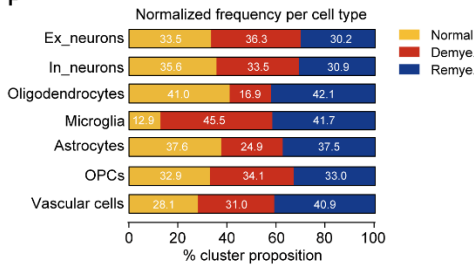


Figure S1. Cluster characterization of cuprizone model in C57BL/6J mice.

(A) Representative electron microscopy (EM) images of corpus callosum (CC) in each condition.

(B) Quantification of percentage of myelinated axons in (A). n=3 mouse brain samples per condition, 5 images per mouse. Data are presented as mean±sd. p value by one-way ANOVA with Tukey's multiple comparisons test. Original magnification, 3000X. Scale bar, 2µm.

(C) Bar plot showing total number of nuclei, median number of genes per nucleus, and median number of UMIs per nucleus of each sample.

(D) Dot plot showing feature genes of each cluster.

(E) UMAP plots showing cell type-specific markers identifying each cluster.

(F) Relative nuclei abundance of each condition per cell type.

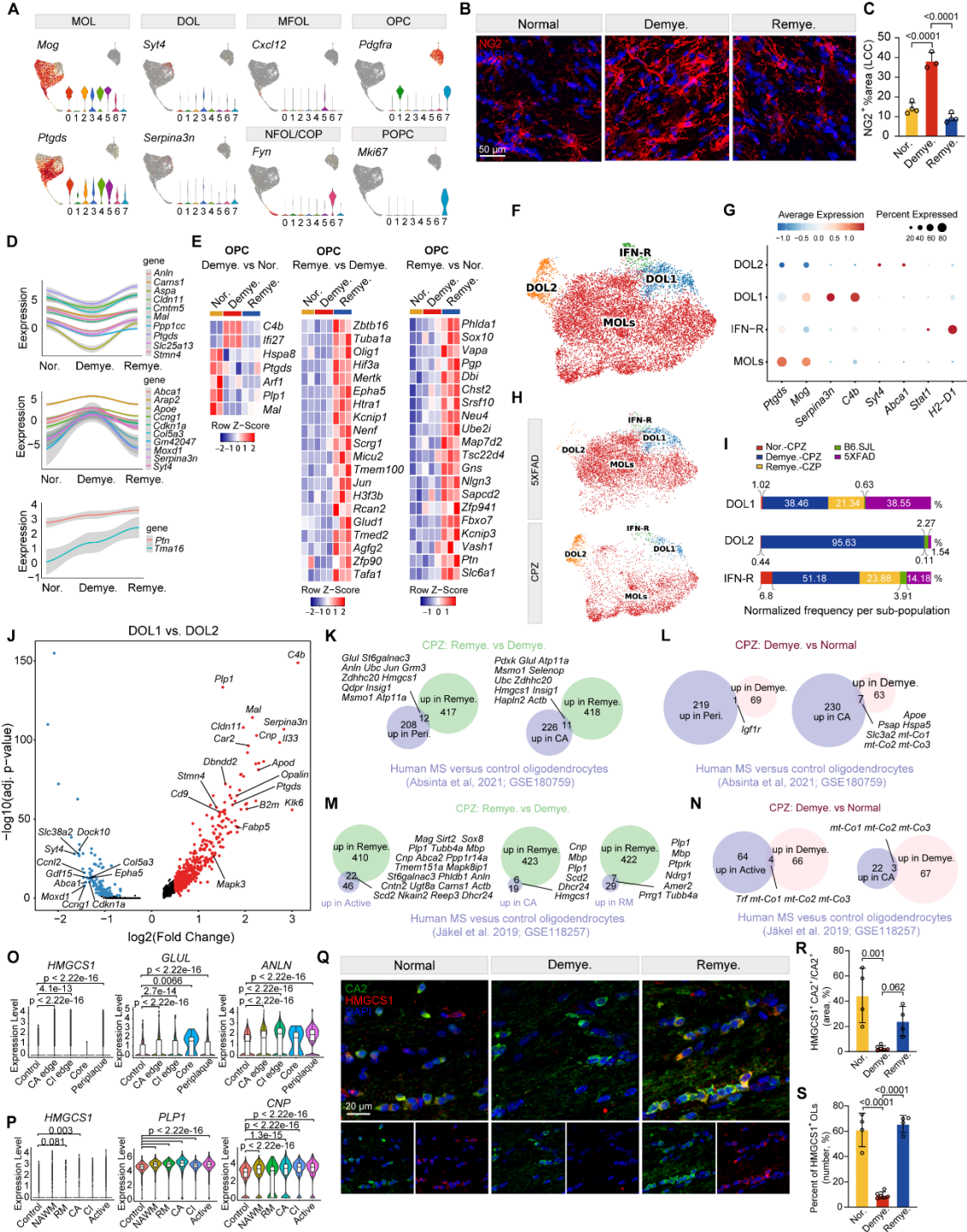


Figure S2. Cluster characterization of oligodendrocyte lineage cells in cuprizone model.

- (A) UMAP plots and violin plots showing feature genes identifying each subcluster.
- (B) Representative IF images of NG2 staining in the lateral CC (LCC) in each condition. NG2, red; DAPI, blue. Scale bar, 50 μ m.
- (C) Quantification of percentage of NG2⁺ area in the LCC from (B). n=3-4 mouse brain samples per condition. Data are presented as mean \pm sd. p value by one-way ANOVA with Tukey's multiple comparisons test.
- (D) Dynamics of average expression of top DEGs in oligodendrocytes (cluster 3 in Figure 1B) over the course of de- and re-myelination. Top 10 genes downregulated (ranked by fold change) in demyelination versus normal (upper). Top 10 genes upregulated (ranked by fold change) in demyelination versus normal (middle). Genes persistently upregulated in demyelination (versus normal) and remyelination (versus demyelination) (bottom).
- (E) Heatmap showing the average gene expression of top DEGs in the OPCs from pairwise comparisons across different conditions. Each column represents one sample. Color scheme represents row z-score.
- (F) UMAP plot showing integration of oligodendrocyte lineage cells from 5XFAD model (GSE202297) and current CPZ dataset using the Seurat integration pipeline.
- (G) Dot plot showing expression of cluster markers of (F).
- (H) UMAP plot split by datasets from (F).
- (I) Relative nuclei contribution of each condition in DOL1, DOL2 and IFN-R.
- (J) Volcano plot showing significant DEGs in DOL1 versus DOL2. log₂(Fold Change)>0.5, adjusted p<0.05, non-parametric Wilcoxon rank sum test, Bonferroni correction.
- (K and L) Venn diagrams of overlap between genes upregulated in various pathological regions of human MS oligodendrocytes (GSE180759) and genes upregulated in oligodendrocytes in the mouse CPZ model: remyelination versus demyelination (K), and demyelination versus normal (L). Overlapping genes are listed on the side. Peri., periplaque; CA, chronic active; CI, chronic inactive; core, lesion core; RM, remyelinated lesions; NAWM, normal-appearing white matter.
- (M and N) Venn diagrams of overlap between genes upregulated in various pathological regions of human MS oligodendrocytes (GSE118257) and genes upregulated in oligodendrocytes in the mouse CPZ model: remyelination versus demyelination (M) and demyelination versus normal (N). Overlapping genes are listed on the side.
- (O and P) Violin plots showing expression of upregulated oligodendrocytes genes in human MS datasets either from GSE180759 (O), or from GSE118257 (P). p value by wilcox test.
- (Q) Representative IF images showing staining of HMGCS1 and CA2 in medial CC in each condition. HMGCS1, red; CA2, green; DAPI, blue. Scale bar, 20 μ m.

(R, S) Ratios of HMGCS1⁺CA2⁺/CA2⁺ areas (R) and numbers (S) across different conditions. n=4-6 biologically independent mouse brain sample per condition. Data are presented as mean±sd. p value by one-way ANOVA with Tukey's multiple comparisons test.

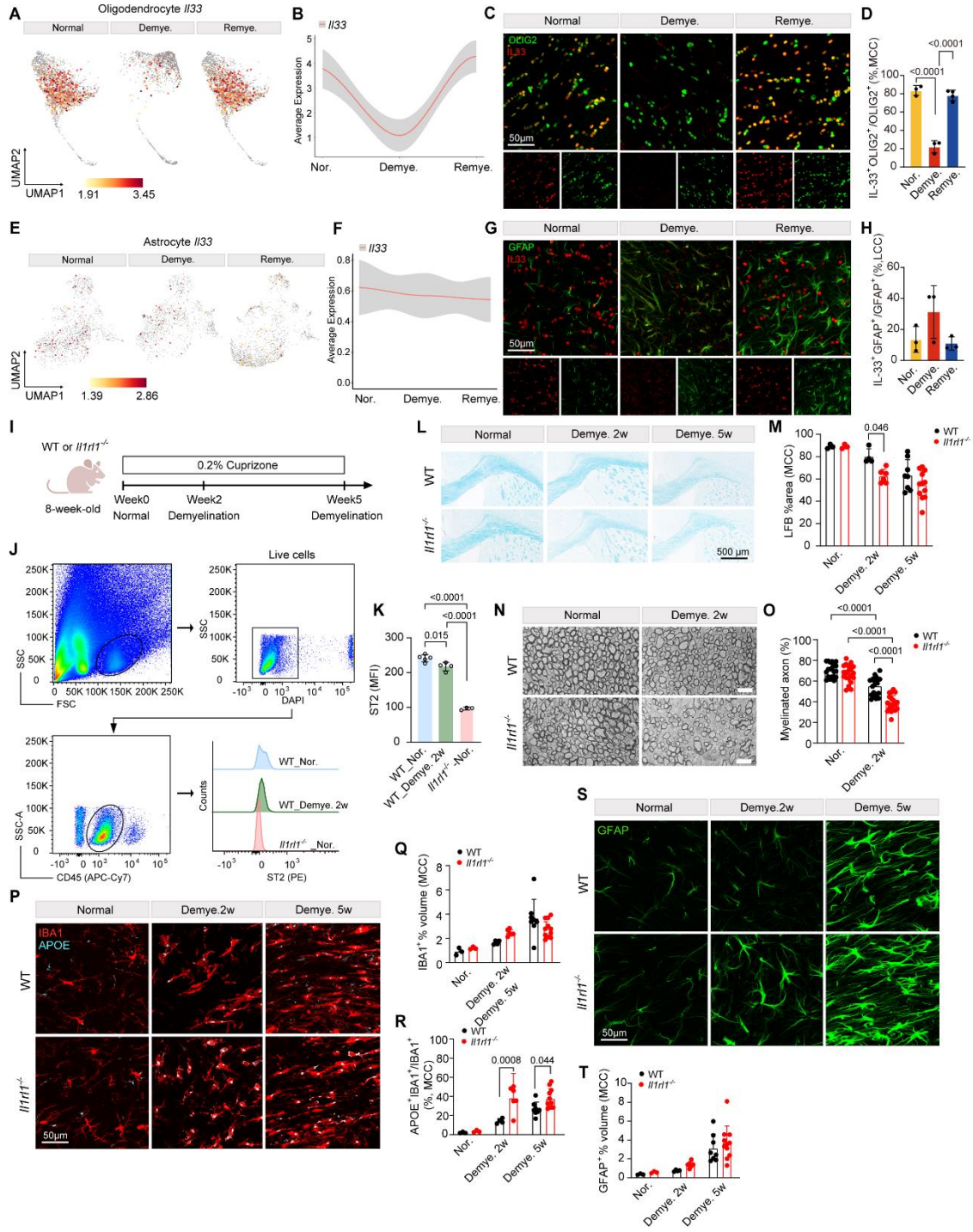


Figure S3. IL-33-ST2 pathway attenuates demyelination.

(A) UMAP plots showing log-normalized gene expression of *Il33* in oligodendrocytes in each condition.

(B) Dynamics of average expression of *Il33* in oligodendrocytes (cluster 3 in Figure 1B) over the course of de- and re-myelination.

(C) Representative IF images of IL-33 and OLIG2 staining in the medial corpus callosum (MCC) in each condition. IL-33, red; OLIG2, green. Scale bar, 50 μ m.

(D) Quantification of IL-33⁺OLIG2⁺/OLIG2⁺ ratio across different conditions. Data are presented as mean \pm sd. n=3-4 mouse brain samples per condition.

(E) UMAP plots showing log-normalized gene expression of *Il33* in astrocytes in each condition.

(F) Dynamics of average expression of *Il33* in astrocytes (cluster 7 in Figure 1B) over the course of de- and re-myelination.

(G) Representative IF images of IL-33 and GFAP staining in the MCC in each condition. IL-33, red; GFAP, green. Scale bar, 50 μ m.

(H) Quantification of IL-33⁺GFAP⁺/GFAP⁺ ratio across different conditions. Data are presented as mean \pm sd. n=3 mouse brain samples per condition.

(I) Schematic diagram of experimental setup. Normal, n=3 WT and 3 *Il1rl1*^{-/-}; Demye. 2w, n=4 WT and 6 *Il1rl1*^{-/-}; Demye. 5w, n=8 WT and 10 *Il1rl1*^{-/-} mice.

(J) Microglial ST2 cell surface expression assessment. Microglia were identified using a light scatter reference, followed by gating on live and CD45^{int} cells. Final histograms show ST2 surface expression in *ex vivo* microglia isolated from WT or *Il1rl1*^{-/-} mice with or without 2-week cuprizone treatment. Histograms represent 3-4 mouse brain samples per condition. FSC, forward scatter; SSC, side scatter; int, intermediate.

(K) Quantification of ST2 mean fluorescence intensity (MFI) of (J). Data are presented as mean \pm sd. n=3-4 mouse brain samples per condition.

(L) Representative LFB staining images of CC of *Il1rl1*^{-/-} and WT mice in each condition. Scale bar, 500 μ m.

(M) Quantification of LFB staining in the MCC from (L). Data are presented as mean \pm sd. n=3-12 mouse brain samples per genotype per condition.

(N) Representative EM images of CC in each condition of *Il1rl1*^{-/-} and WT mice, treated with or without 2-week cuprizone. Original magnification, 3000X. Scale bar, 2 μ m.

(O) Quantification of percentage of myelinated axons in (N). n=4 mouse brain samples per condition, 5 images per mouse. Each dot represents one image. Data are presented as mean \pm sd.

(P) Representative IF images of APOE and IBA1 staining in the MCC of *Il1rl1*^{-/-} and WT mice in each condition. IBA1, red; APOE, cyan. Scale bar, 50 μ m.

(Q) Quantification of IBA1⁺ volume in MCC across different conditions. Data are presented as mean±sd. n=3-11 mouse brain samples per genotype per condition.

(R) Quantification of APOE⁺IBA1⁺/IBA1⁺ ratio across different conditions. Data are presented as mean±sd. n=3-11 mouse brain samples per genotype per condition.

(S) Representative IF images of GFAP staining in the MCC in *Il1r1^{-/-}* and WT mice in each condition. GFAP, green. Scale bar, 50µm.

(T) Quantification of GFAP⁺ volume in MCC across different conditions. Data are presented as mean±sd. n=3-11 mouse brain samples per genotype per condition. p value by one-way ANOVA with Tukey's multiple comparisons test in (D, H, K). P value by two-way ANOVA with Tukey's multiple comparisons test in (M, O, Q, R, and T).

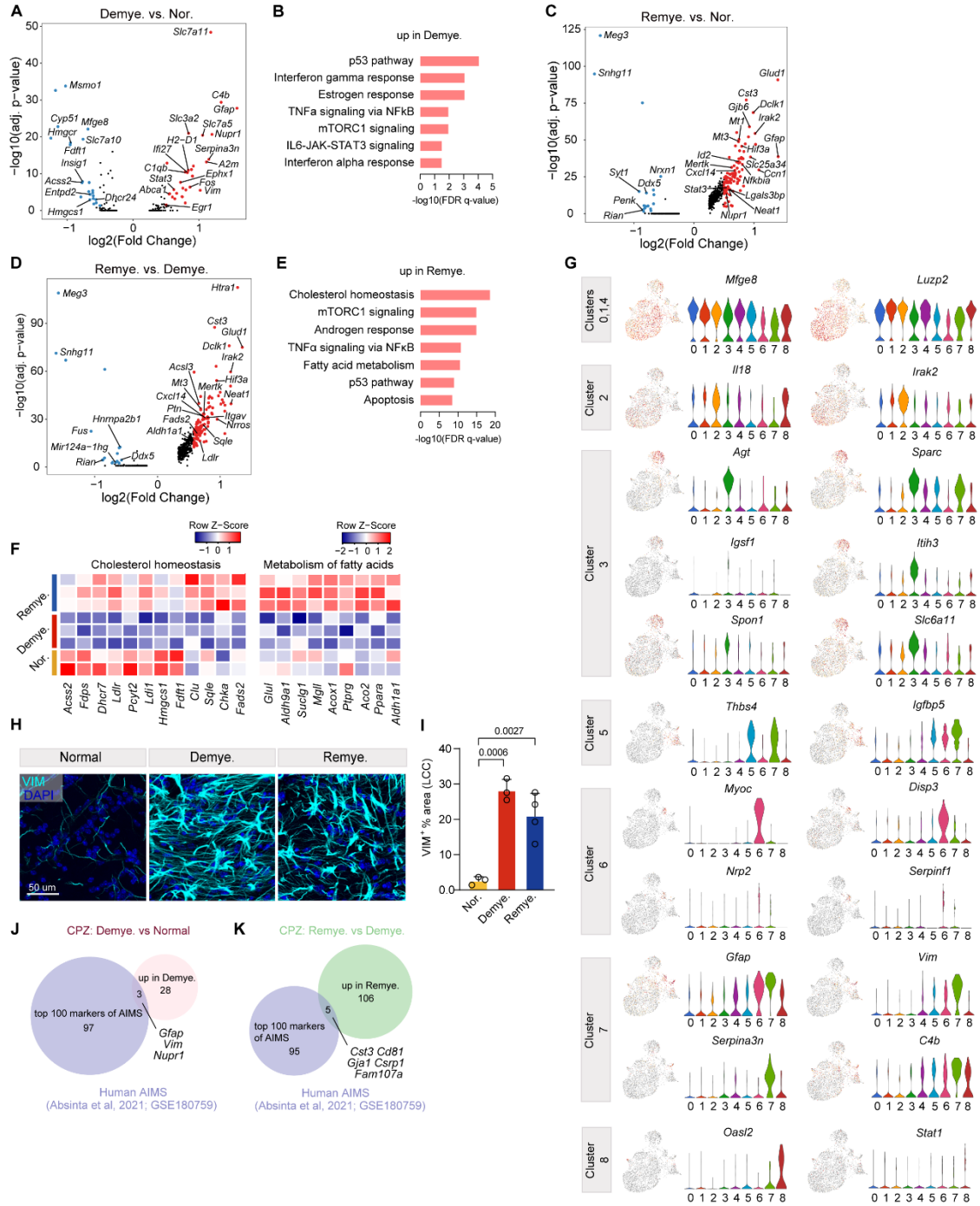


Figure S4. Characterization of astrocyte cluster in cuprizone model.

(A) Volcano plot showing significant DEGs in astrocytes between demyelination versus normal. $\log_2(\text{Fold Change}) > 0.5$, adjusted $p < 0.05$, non-parametric Wilcoxon rank sum test, Bonferroni correction.

(B) GSEA of genes upregulated in astrocytes in demyelination versus normal. $\log_2(\text{Fold Change}) > 0.25$, adjusted $p < 0.05$.

(C and D) Volcano plot showing significant DEGs in astrocytes by pairwise comparisons between remyelination versus normal (C), or remyelination versus demyelination (D). $\log_2(\text{Fold Change}) > 0.5$, adjusted $p < 0.05$, non-parametric Wilcoxon rank sum test, Bonferroni correction.

(E) GSEA of genes upregulated in astrocytes in remyelination versus demyelination. $\log_2(\text{Fold Change}) > 0.25$, adjusted $p < 0.05$.

(F) Heatmap showing average expression of genes in cholesterol homeostasis and metabolism of fatty acid pathways from (E).

(G) UMAP plots and violin plots of feature genes identifying each subcluster.

(H) Representative IF images of VIM staining in the LCC in each condition. DAPI, blue; VIM, cyan. Scale bar, 50 μm .

(I) Quantification of percentage of VIM⁺ area in LCC. $n=3$ mice in normal, 3 in demyelination, and 4 in remyelination condition. Data are presented as mean \pm sd. p value by one-way ANOVA with Tukey's multiple comparisons test.

(J and K) Venn diagrams of overlap between top 100 markers of 'astrocytes inflamed in multiple sclerosis' (AIMS, GSE180759) and genes upregulated in astrocytes in the mouse CPZ model: demyelination versus normal (J), and remyelination versus demyelination (K). Overlapping genes are listed on the side.

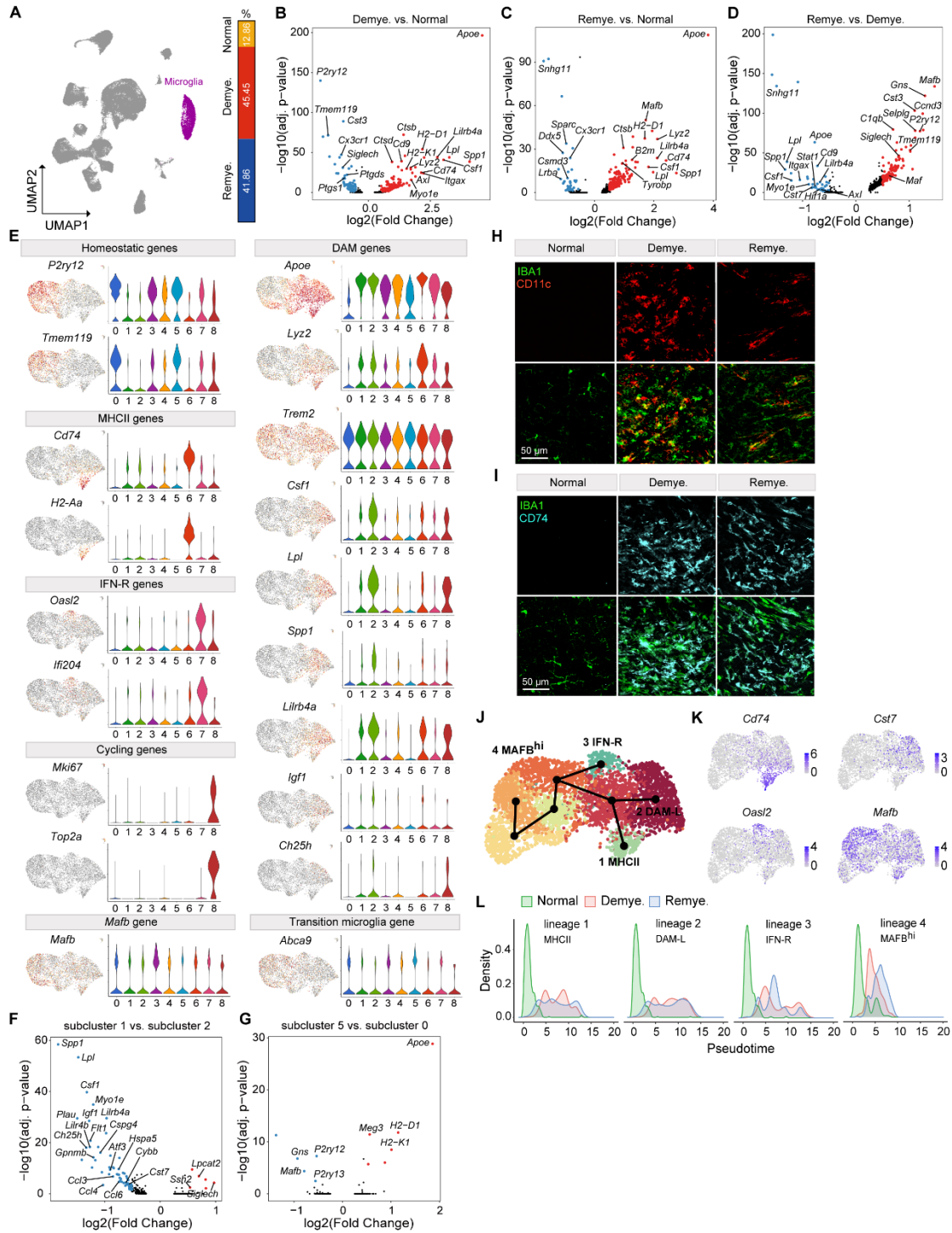


Figure S5. Characterization of microglia cluster in cuprizone model.

(A) UMAP plot showing the microglia cluster (cluster 4 in Figure 1B), and relative frequency across different conditions.

(B-D) Volcano plot showing significant DEGs in microglia by pairwise comparisons between demyelination versus normal (B), remyelination versus normal (C), or remyelination versus demyelination (D). $\log_2(\text{Fold Change}) > 0.5$, adjusted $p < 0.05$, non-parametric Wilcoxon rank sum test, Bonferroni correction.

(E) UMAP plots and violin plots showing feature genes identifying each subcluster.

(F) Volcano plot showing significant DEGs between subcluster1 and subcluster2. $\log_2(\text{Fold Change}) > 0.5$, adjusted $p < 0.05$, non-parametric Wilcoxon rank sum test, Bonferroni correction.

(G) Volcano plot showing significant DEGs between subcluster5 and subcluster0. $\log_2(\text{Fold Change}) > 0.5$, adjusted $p < 0.05$, non-parametric Wilcoxon rank sum test, Bonferroni correction.

(H) Representative IF images showing colocalization of CD11c and IBA1 in the LCC in each condition. IBA1, green; CD11c, red. Scale bar, 50 μm .

(I) Representative IF images showing colocalization of CD74 and IBA1 in the LCC in each condition. IBA1, green; CD74, cyan. Scale bar, 50 μm .

(J) UMAP plot showing the projection of the four trajectories by slingshot on microglia clusters (subcluster 8 was excluded from this analysis).

(K) UMAP plots showing expression of marker genes of each trajectory in (J).

(L) Histograms showing the distribution of microglia nuclei from each condition along the four trajectories. HM, homeostatic microglia; TM, transition microglia; DAM-L, DAM-like; IFN-R, interferon responsive; PM, proliferating microglia; Mito, mitochondria.

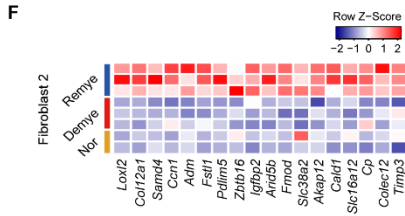
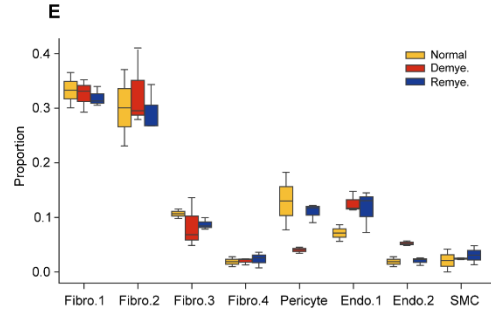
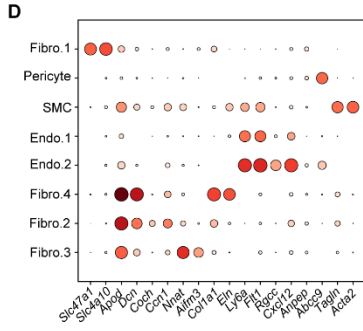
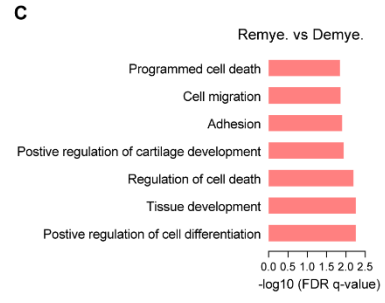
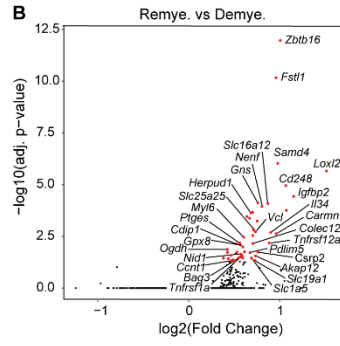
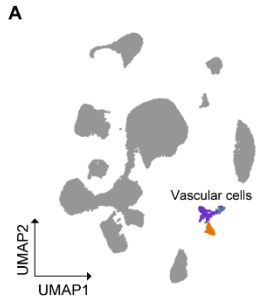


Figure S6. Transcriptional changes in vascular cells.

(A) UMAP plot showing the vascular cell clusters (clusters 13, 14 and 18 in Figure 1B).

(B) Volcano plot showing DEGs in remyelination versus demyelination of all vascular cells. $\log_2(\text{Fold Change}) > 0.5$, adjusted $p < 0.05$, non-parametric Wilcoxon rank sum test, Bonferroni correction.

(C) GSEA of genes upregulated in vascular cells in remyelination versus demyelination $\log_2(\text{Fold Change}) > 0.25$, adjusted $p < 0.05$.

(D) Dot plot showing the feature genes for each subcluster.

(E) Sub-cluster compositional analysis across different conditions. No statistically credible change was found as tested by scCODA. $n=2$ mice in normal, 3 in demyelination, and 3 in remyelination condition.

(F) Heatmap showing average expression of top DEGs in the Fibro.2 cluster ($\log_2(\text{Fold Change}) > 0.5$, adjusted $p < 0.05$) in remyelination versus demyelination in each sample. Color scheme represents row z-score.

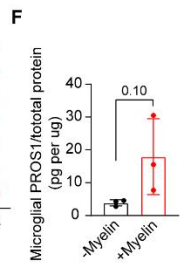
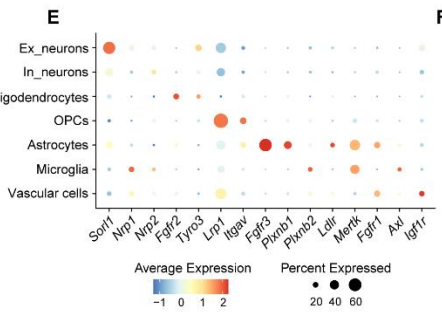
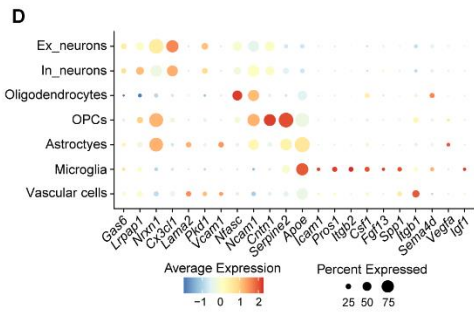
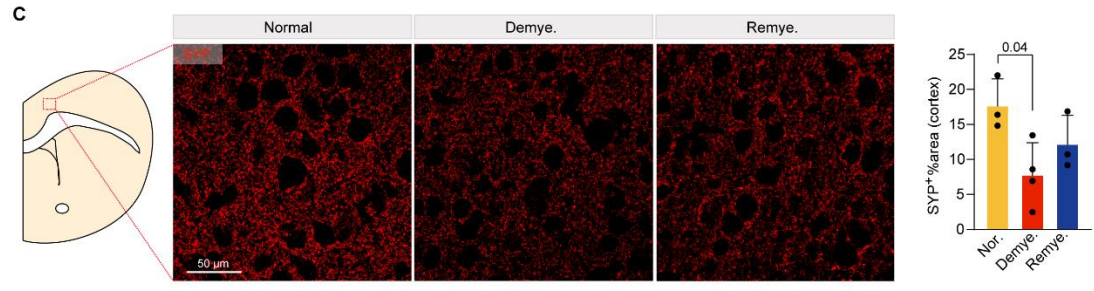
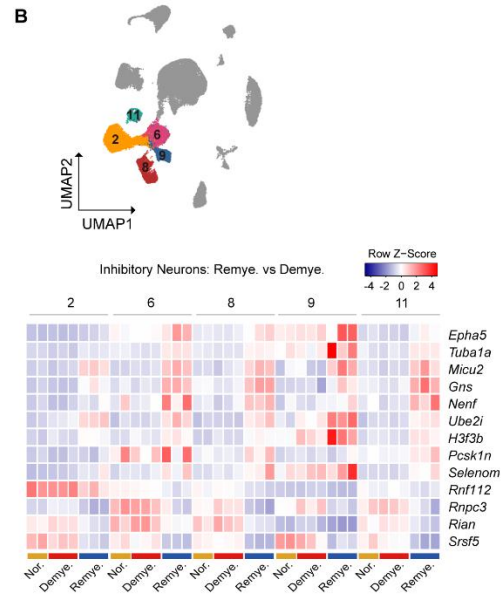
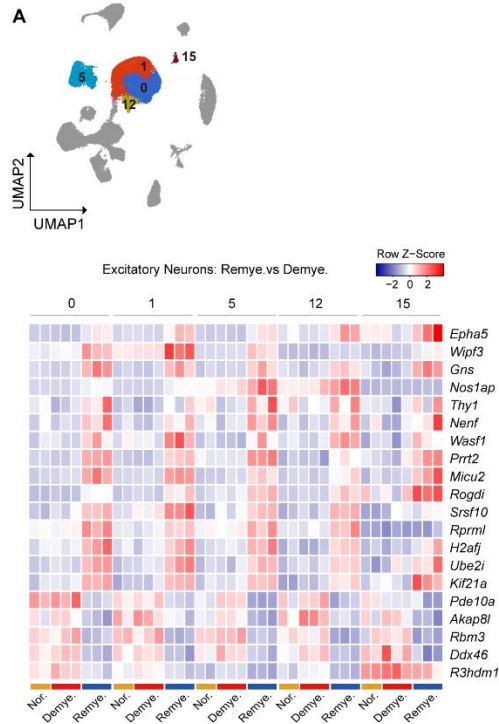


Figure S7. Transcriptional changes in neurons, as well as ligands and receptors predicted by NicheNet analysis.

(A and B) Heatmap showing average gene expression of top DEGs in each cluster of excitatory neurons (A) and inhibitory neurons (B). Each column represents one mouse. Color scheme represents row z-score. UMAP plots on the top show the different subclusters of neurons.

(C) Representative immunofluorescence images of Synaptophysin (SYP) in the cortex in each condition and quantification of percentage of SYP⁺ area in the cortex. SYP, red. Cartoon on the left showing the region of interest. n=3-4 mouse brain samples per condition. Data are presented as mean±sd. p value by one-way ANOVA with Tukey's multiple comparisons test. Scale bar, 50µm.

(D and E) Dot plot of ligands (D) and receptors (E) identified by NicheNet analysis showing their cell type-specific gene expression.

(F) Bar graph of PROS1 protein level in primary microglia lysates by ELISA, normalized to total protein level. Data are presented as mean±sd. p value by Student's *t* test.

Figure S8. Cluster characterization of WT and *Trem2*^{-/-} mice in the cuprizone model.

(A) Schematic diagram of experimental strategy.

(B) Representative EM images of CC in each condition. Deposition of myelin debris (black arrowheads) and axonal spheroids (red arrowheads) are indicated in *Trem2*^{-/-} mice. Original magnification, 3000x. Scale bar, 2 μ m.

(C and D) Quantification of myelination states in (B) measured by percentage of myelinated axons (C) and G-ratios (D). n=3-4 mouse brain samples per genotype per condition, 5-10 images per mouse. Data are presented as mean \pm sd. p value by two-way ANOVA with Tukey's multiple comparisons test.

(E) Representative IF images of OLIG2 staining in MCC in *Trem2*^{-/-} and WT mice in each condition. Scale bar, 50 μ m.

(F) Quantification of OLIG2⁺ density in MCC across different conditions. n=3-5 mouse brain samples per genotype per condition. Data are presented as mean \pm sd. p value by two-way ANOVA with Tukey's multiple comparisons test.

(G) Bar plot showing total number of nuclei, median number of genes, and median number of UMIs of each sample.

(H) Dot plot showing feature genes of each cluster.

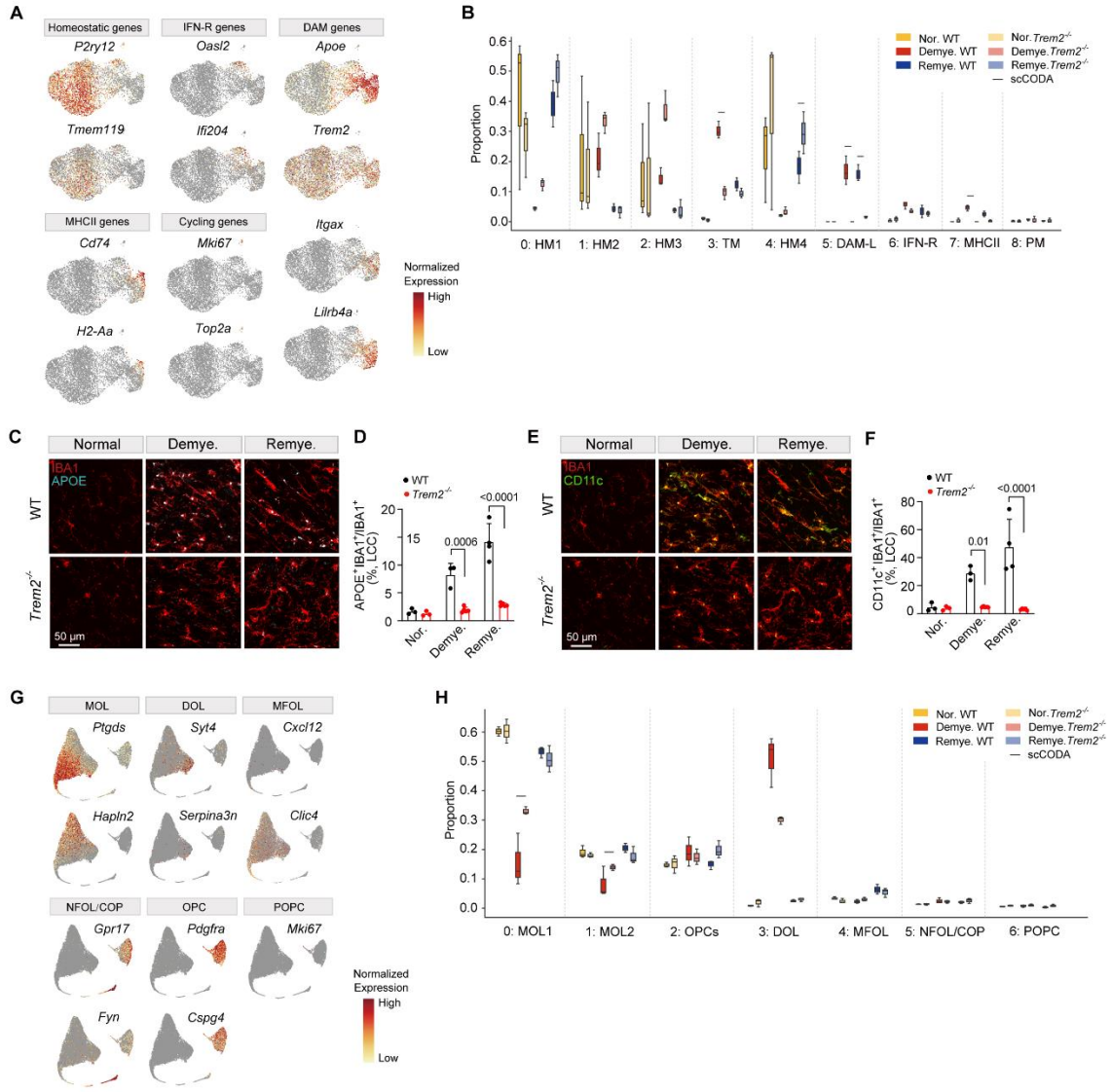


Figure S9. TREM2 deficiency impairs microglia and oligodendrocyte responses to CPZ-induced myelin alterations.

- (A) UMAP plots showing feature genes identifying each microglial subcluster.
- (B) Sub-cluster compositional analysis between WT to *Trem2*^{-/-} microglia in each condition. Statistically credible changes, as tested by scCODA, are denoted with bars on top.
- (C) Representative IF images of APOE and IBA1 staining in the LCC of *Trem2*^{-/-} and WT mice in each condition. APOE, cyan; IBA1, red. Scale bar, 50µm.
- (D) Quantification of APOE⁺IBA1⁺/IBA1⁺ ratio in LCC across different conditions. n=3-5 biologically independent mouse brain sample per genotype per condition. Data are presented as mean±sd. p value by two-way ANOVA with Tukey's multiple comparisons test.
- (E) Representative IF images of CD11c and IBA1 staining in the LCC of *Trem2*^{-/-} and WT mice in each condition. CD11c, green; IBA1, red. Scale bar, 50µm.
- (F) Quantification of CD11c⁺IBA1⁺/IBA1⁺ ratio in LCC across different conditions. n=3-5 mouse brain samples per genotype per condition. Data are presented as mean±sd. p value by two-way ANOVA with Tukey's multiple comparisons test.
- (G) UMAP plots showing feature genes identifying each oligodendrocyte lineage subcluster.
- (H) Sub-cluster compositional analysis between WT to *Trem2*^{-/-} oligodendrocyte lineage nuclei in each condition. Statistically credible changes, as tested by scCODA, are denoted with bars on top.